Temporal Modulation of Traveling Waves

I. Rehberg,[a] S. Rasenat,[a] J. Fineberg, M. de la Torre Juarez,[a] and V. Steinberg[b]
Department of Nuclear Physics, Weizmann Institut, 76100 Rehovot, Israel
(Received 6 September 1988)

It is demonstrated that traveling waves lose stability with respect to standing waves under the influence of a spatially homogeneous temporal modulation in three different experimental systems. A phase diagram consistent with a recent theoretical prediction is presented.

PACS numbers: 47.25.Ae, 47.20.−k

There has been much recent experimental and theoretical interest in experimentally well controlled systems exhibiting an oscillatory instability as a first bifurcation. They can be quantitatively described by a generalized Ginzburg-Landau (GGL) equation with complex coefficients. One of these systems, convective binary mixtures, has attracted a great deal of attention because of the possibility to perform high-resolution measurements of temporal and spatial pattern dynamics.[1] Similar oscillatory instabilities were found in Taylor-Couette flow[2] and in electrohydrodynamic convection[3,4] of nematic liquid crystals. In all of these systems nonlinear coupling between the left- and right-propagating waves leads to the stabilization of traveling waves (TW) with respect to standing waves (SW). Recently, however, it was predicted that a spatially uniform temporal modulation (as well as a steady-spatial modulation) of TW stabilizes the SW pattern.[5,6] From a theoretical point of view, the effect of a small perturbation of the time translational symmetry on a spatiotemporal pattern is an interesting question. From an experimental point of view, this simple realization of SW offers another system described by the GGL equation, where basic questions like the stability of SW and topological defects associated with them[7] can be studied. Moreover, modulation leads to a phase diagram containing an experimentally easily accessible codimension-two point,[5] and it offers the possibility to measure the coefficients of the GGL equation by simply analyzing the bifurcation lines.[8] This paper presents the realization of stable SW in three different physical systems.

We measured the onset of electrohydrodynamic convection in a cell of 15-μm thickness as described in Ref. 4 using the nematic liquid crystal Merck Phase V. The width and the length of the channel were 0.5 mm and 3 cm, respectively, thus forming an aspect ratio of 1:33:2000. Figure 1 shows the corresponding phase diagram. The driving voltage at which the motionless ground state loses stability with respect to convective motion, V_c, is plotted as a function of the driving frequency. Below 375 Hz steady Williams rolls set in.

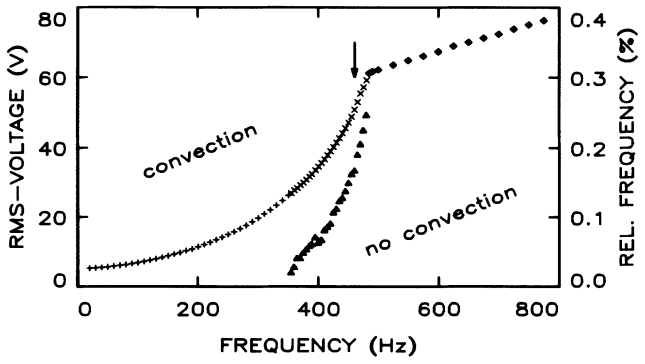

FIG. 1. Phase diagram for the onset of convection in the nematic liquid crystal Phase V. The plus signs indicate the onset of steady convection; crosses, the onset of TW; triangles, the frequency of TW normalized by the cutoff frequency; and diamonds, the onset of dielectric convection. The arrow points to the working frequency used in Figs. 2–5.

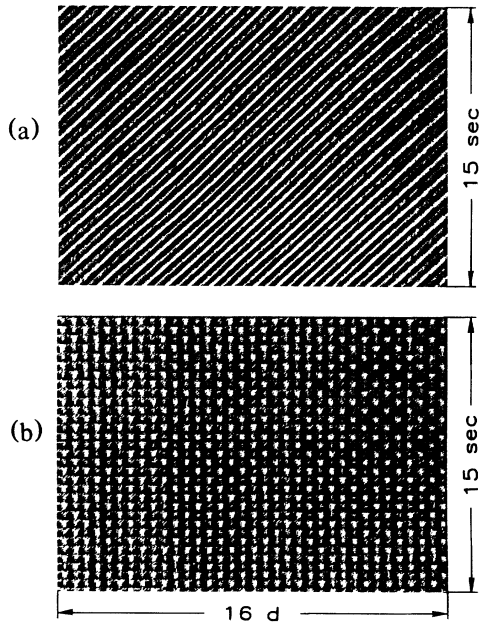

FIG. 2. (a) TW at $R=1.01$, and (b) SW at $R_0=1.0$, $b=2\%$, $\Delta\omega=0\%$. The intensity along a line of length $16d$ is measured every 40 msec. 400 lines are plotted on top of each other with five grey levels.

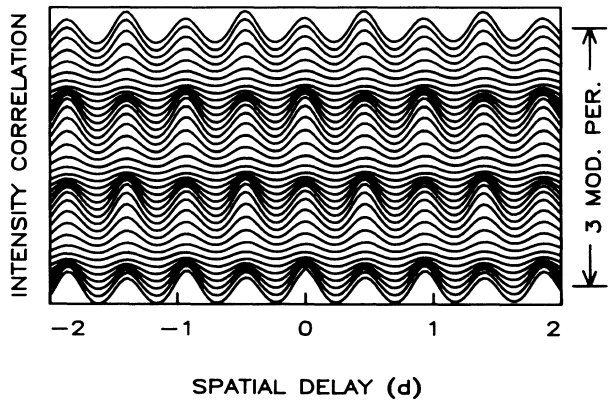

FIG. 3. The structure function of a standing wave based on the data shown in Fig. 2(b). The temporal period of the pattern is demonstrated to be half the period of the modulation. The lack of decay in space and time indicates the stability of the SW pattern.

They start as traveling rolls between 375 and 487 Hz, the area of interest for the measurements presented here. The arrow points to the frequency where the measurements shown in Figs. 2–5 are performed. The triangles indicate the frequency of the TW at the onset of convection, ω_h, normalized by 487 Hz, the cutoff frequency of the driving ac voltage.

The upper part of Fig. 2 shows the existence of TW at a driving frequency of 425 Hz and a rms voltage of 50 V corresponding to a reduced driving voltage, $R=V/V_c$, of 1.01. Here the intensity along a line perpendicular to the roll axis is measured every 40 msec, and 400 temporally consecutive lines are plotted. Unlike in Ref. 3 these TW do not look like patches at onset, but are spatially homogeneous. Also unlike Ref. 3, in our system the TW frequency decreases as the amplitude increases, indicating that our measurements are done in a different regime of the phase diagram. The lower part of Fig. 2 demonstrates the fact that TW lose stability with respect to SW under the influence of a temporal modulation of R described by $R(t)=R_0+b\sin(\omega t)$ with the modulation amplitude b measured in units of V_c. In Fig. 2, $b=2\%$ and $R_0=1$.

For quantitative analysis of the waves the intensity structure function[9] $S(\Delta x,\Delta t)=\langle[I(x,t)-I(x+\Delta x, t+\Delta t)]^2\rangle_{x,t}$ is a useful tool. The structure function for the data presented in Fig. 2(b) is shown in Fig. 3. No difference for positive and negative values of the "spatial delay," Δx, are visible, indicating that the left and right traveling waves have the same amplitude. No hint of a decay of the structure function is visible in space or time, indicating the SW to be spatially and temporarily homogeneous. The spatial period of the pattern is about 0.9 unit of the cell height—unlike in thermal convection where the wavelength $\lambda\approx 2d$. The higher maxima correspond to upflow and the lower maxima to downflow.[10] Within one modulation period upflow and downflow exchange their position, thus demonstrating that the tem-

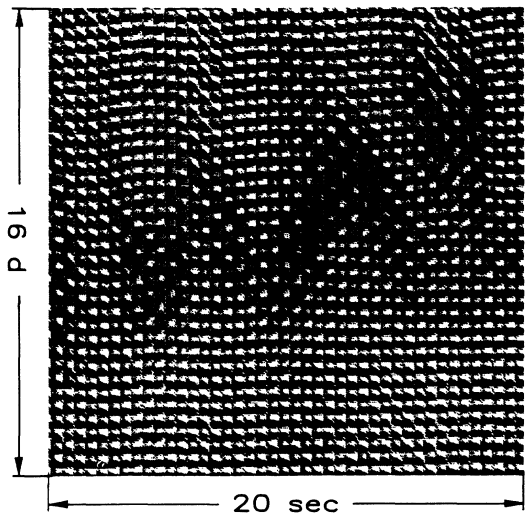

FIG. 4. At $R_0=1.04$ and a modulation $b=2\%$, $\Delta\omega=0\%$, the SW are unstable. The figure shows left and right traveling TW accompanied by defects.

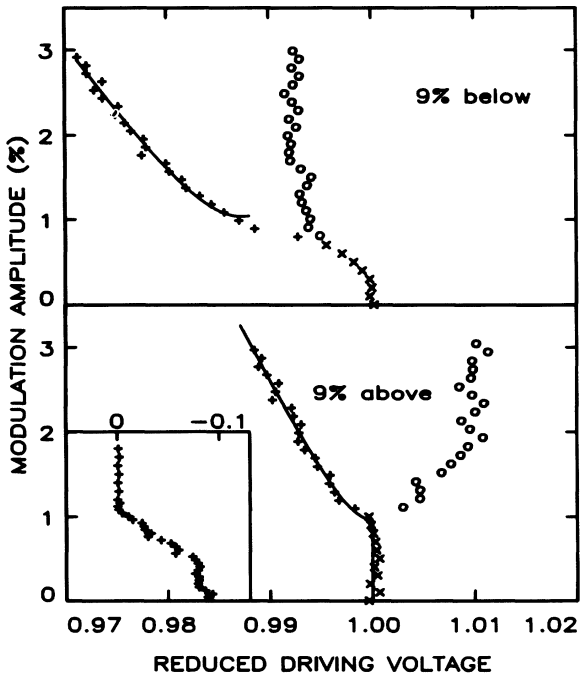

FIG. 5. Bifurcation diagram with a modulation frequency of 9% above and 9% below the linear frequency. Crosses and plus signs indicate the voltage where the ground state loses stability to TW and SW, respectively. The circles indicate the secondary instability where TW loses stability. The solid lines are fits by the theoretically predicted curve for the onset of convection. Inset: The frequency difference between the TW and the modulation frequency.

poral period of the flow field is twice the period of the modulation.

Increasing the amplitude of the driving R_0 at a constant modulation b leads to an instability of the standing-wave pattern. Figure 4 shows a typical spatiotemporal pattern observed beyond the transition. Modulated TW together with defects can be seen in parts of the figure. We were unable to find a region of the phase space beyond the transition line (circles in Fig. 5 below) where a defect-free pattern existed.

We measured the onset of convection [either as standing (plus signs) or traveling waves (crosses)] and the instability line for the standing waves (circles) as a function of the reduced driving voltage R and the modulation amplitude b. The result is shown in Fig. 5 for two values of the modulation frequency, ω_m. One value shown is well above ($\Delta\omega=\omega_m/2\omega_h-1=9\%$) the linear frequency ω_h of unmodulated TW and one is 9% below that value. For small modulation amplitudes ($b<1\%$) convection sets in as TW. At about 1% the character of the waves changes to SW, which are phase locked to the modulation frequency as demonstrated by the inset where the frequency difference between the driving and the velocity of one TW component is plotted as a function of the modulation amplitude b. This phase diagram is in agreement with the theoretical prediction,[5] where it was also pointed out that the Takens-Bogdanow codimension-two point, where the difference between the driving frequency and the waves ceases, is analogous to the one obtained in the convection of binary mixtures[1] at the transition from oscillatory to steady convection. The shape of the linear instability line can be calculated on the basis of symmetry arguments[5,8] to be the hyperbola $b^2=C^2[(R-1-B)^2+A^2]$. The solid lines in Fig. 5 show fits of the SW onset by this curve (lower curve: $A=0.39\%$, $B=0.024\%$, $C=2.4$; upper curve: $A=0.66\%$, $B=-0.12\%$, $C=1.7$). Note that the position of the saddle of the hyperbola, B, changes sign when changing the sign of the detuning, in agreement with the prediction. The theory predicts hysteresis for the onset to SW to happen either below or above the linear frequency of the TW—but being based on general symmetry arguments it cannot predict which side. Measuring the resonance curve gives a hint about the location of the hysteresis. It should appear at the side where the curve has a tendency for folding. Based on measured resonance curves we expect the hysteresis to occur in the upper figure. The tricritical point where hysteresis sets in is presumably located around $R=0.985$, where the data begin to deviate from the fit. We were not able to resolve the hysteresis, however, possibly because of a lack of homogeneity of the cell. The effect of spatial inhomogeneities of extended systems on the problem of resolving a small hysteresis has been treated numerically.[11] Based on these calculations one could estimate our resolution for hysteresis to be about $\Delta\epsilon=0.001$, which is about of the order of magnitude that we would expect for the hysteresis loop when comparing Fig. 5 to Fig. 3 of Ref. 5.

To demonstrate the universality to be expected from a theory based on symmetry arguments, we performed analogous modulation experiments in two additional systems exhibiting traveling waves, namely, (i) thin cells of the nematic liquid crystal N-(p-methoxybenzylidine)-p-butylaniline (MBBA) and (ii) binary-mixture convection. For (i) the bifurcation was demonstrated to be forward[4] while for (ii) it is known to be backwards.[1,12] In both cases modulation stabilized the SW relative to the TW (which are obtained when no modulation is present) as demonstrated by Figs. 6 and 7. The cell used for MBBA had the same aspect ratio as the Phase-V cell described above. The corresponding phase diagram is present elsewhere[4] and differs from Fig. 1 mostly in the aspect that the primary bifurcation is to TW for any

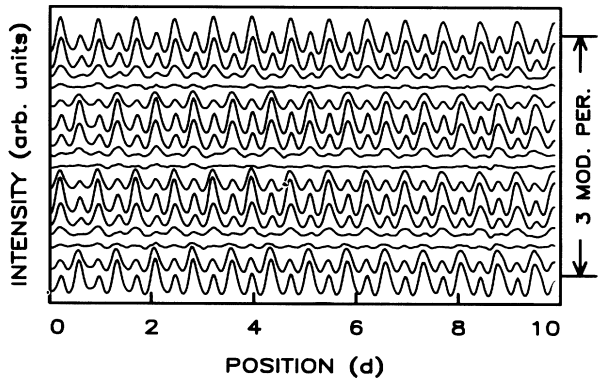

FIG. 6. SW in MBBA. $R_0=0.99$, $b=6\%$, $\Delta\omega=-7\%$. The intensity along a line is measured 10 times within a modulation period, and the results are plotted on top of each other. High intensity maxima correspond to upflow, smaller maxima to downflow.

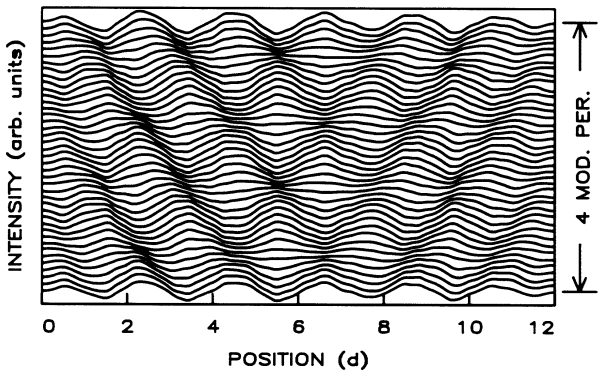

FIG. 7. SW in binary-mixture convection in a small box. $R_0=1.001$, $b=1\%$, $\Delta\omega=0\%$. Intensity maxima correspond to downflow, minima to upflow.

driving frequency between 0 and the cutoff frequency of 450 Hz. The data for Fig. 6 were taken at a driving voltage of $R_0=0.991$ (35 V, 350 Hz), with a modulation amplitude $b=6\%$ and $\Delta\omega=-7\%$.

The convection cell used for the binary-mixture experiment had an aspect ratio of height:width:length of 1:4:12.[13] A 26% ethanol-water mixture was used as the working fluid, at a reduced driving temperature of $R_0=T/T_c=1.001$, detuning $\Delta\omega=0\%$, and a modulation amplitude of 1%. Unlike in the very long cells described above, the boundaries lead to a spatial modulation of left and right traveling waves throughout the cell—they grow when traveling through the cell and are reflected at the boundaries with a reflection coefficient smaller than 1.[14] This fact is demonstrated in Fig. 7. In the middle of the cell the pattern looks like a standing wave, because left and right traveling waves have the same magnitude. In the left-hand part of the cell, the left traveling wave overcomes the amplitude of the right traveling wave and vice versa on the right-hand side of the cell.

In summary, the predictions of a general theory based on stability arguments for oscillatory pattern-forming instabilities have been verified qualitatively and semiquantitatively. Our present work concentrates on the quantitative aspect of the problem, namely to use it as a tool to measure the coefficients of the GGL equation[8] in the first system described.

The stay of I.R. and S.R. at the Weizmann Institute was supported by the Minerva Foundation. We would like to thank H. Riecke for an early draft of Ref. 8, and many helpful hints.

[a]Permanent address: Physikalisches Institut, Universität, Bayreuth, D-8580 Bayreuth, West Germany.

[b]Present address: Center for Nonlinear Studies, LANL, Los Alamos, NM 87545.

[1]G. Ahlers, D. S. Cannell, and R. S. Heinrichs, in *Chaos 87, International Conference on the Physics of Chaos and Systems Far from Equilibrium,* edited by M. Duong-van (North-Holland, Amsterdam, 1987); P. Kolodner, A. Passner, H. L. Williams, and C. M. Surko, *ibid.*; V. Steinberg, E. Moses, and J. Fineberg, *ibid.*

[2]C. D. Andereck, S. S. Liu, and H. L. Swinney, J. Fluid. Mech. **164**, 155 (1986); R. Tagg and H. L. Swinney, unpublished.

[3]A. Joets and R. Ribotta, Phys. Rev. Lett. **60**, 2164 (1988).

[4]I. Rehberg, S. Rasenat, and V. Steinberg, to be published.

[5]H. Riecke, J. D. Crawford, and E. Knobloch, to be published.

[6]D. Walgraef, to be published.

[7]P. Coullet, C. Elphick, L. Gil, and J. Lega, Phys. Rev. Lett. **59**, 884 (1987); P. Coullet, L. Gil, and J. Lega, to be published; L. Gil, J. Lega, and J. L. Meunier, to be published.

[8]H. Riecke and J. D. Crawford, to be published.

[9]E. O. Schulz-DuBois and I. Rehberg, Appl. Phys. **24**, 323 (1981).

[10]S. Rasenat, G. Hartung, B. L. Winkler, and I. Rehberg, to be published.

[11]Barbara J. A. Zielinska, to be published.

[12]W. Schöpf and W. Zimmerman, to be published.

[13]Details of the convection apparatus used are given in J. Fineberg, E. Moses, and V. Steinberg, Phys. Rev. Lett. **61**, 838 (1988).

[14]M. C. Cross, Phys. Rev. Lett. **57**, 2935 (1986); P. Kolodner, C. M. Surko, A. Passner, and H. L. Williams, Phys. Rev. A **36**, 2499 (1987).

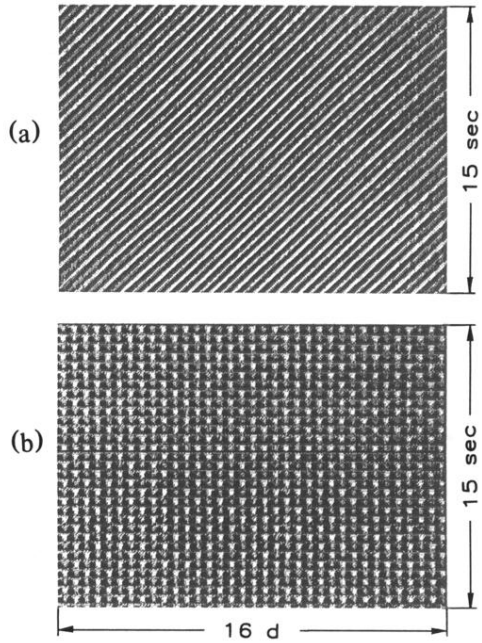

FIG. 2. (a) TW at $R=1.01$, and (b) SW at $R_0=1.0$, $b=2\%$, $\Delta\omega=0\%$. The intensity along a line of length $16d$ is measured every 40 msec. 400 lines are plotted on top of each other with five grey levels.

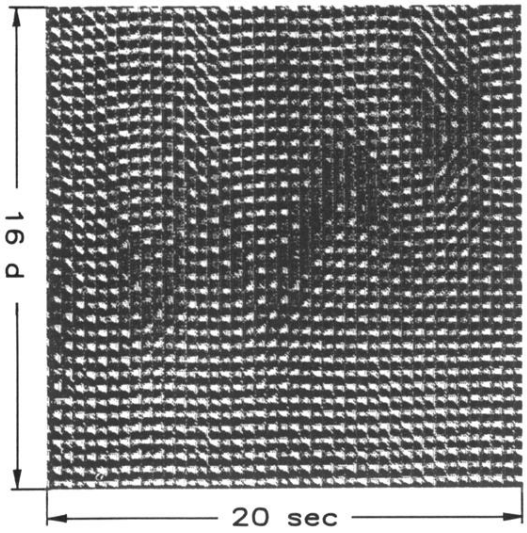

FIG. 4. At $R_0 = 1.04$ and a modulation $b = 2\%$, $\Delta\omega = 0\%$, the SW are unstable. The figure shows left and right traveling TW accompanied by defects.